ELSEVIER

Journal of Structural Geology 30 (2008) 341–353

JOURNAL OF STRUCTURAL GEOLOGY

www.elsevier.com/locate/jsg

# Power-law viscous materials for analogue experiments: New data on the rheology of highly-filled silicone polymers

D. Boutelier*, C. Schrank, A. Cruden

*Department of Geology, Earth Sciences Centre, University of Toronto, 22 Russell Street, Toronto, ON M5S 3B1, Canada*

Received 6 April 2007; received in revised form 5 September 2007; accepted 12 October 2007
Available online 19 November 2007

**Abstract**

The selection of appropriate analogue materials is a central consideration in the design of realistic physical models. We investigate the rheology of highly-filled silicone polymers in order to find materials with a power-law strain-rate softening rheology suitable for modelling rock deformation by dislocation creep and report the rheological properties of the materials as functions of the filler content. The mixtures exhibit strain-rate softening behaviour but with increasing amounts of filler become strain-dependent. For the strain-independent viscous materials, flow laws are presented while for strain-dependent materials the relative importance of strain and strain rate softening/hardening is reported. If the stress or strain rate is above a threshold value some highly-filled silicone polymers may be considered linear visco-elastic (strain independent) and power-law strain-rate softening. The power-law exponent can be raised from 1 to ~3 by using mixtures of high-viscosity silicone and plasticine. However, the need for high shear strain rates to obtain the power-law rheology imposes some restrictions on the usage of such materials for geodynamic modelling. Two simple shear experiments are presented that use Newtonian and power-law strain-rate softening materials. The results demonstrate how materials with power-law rheology result in better strain localization in analogue experiments.


*Keywords:* Rheology; Analogue modelling; Power law creep; Strain localization

## 1. Introduction

Plate tectonics implies the operation of efficient strain localization processes in order to produce and maintain lithospheric shear zones. Localization phenomena can be generated or initiated within the brittle part of both oceanic lithosphere and continental crust as well as in the uppermost continental lithospheric mantle that is potentially brittle (Brace and Kohlstedt, 1980). Strain localization is also observed in ductile shear zones but the mechanisms contributing to this process are not yet completely understood. Localization in the ductile regime may be promoted by strain weakening mechanisms such as dynamic recrystallization or shear heating (Poirier, 1980; White et al., 1980; Montési and Zuber, 2002). However, the weakening functions associated with these mechanisms are still debated (Rutter, 1999; De Bresser et al., 2000; Montési and Hirth, 2003). In the lowermost mantle lithosphere, viscous creep by dislocation glide is believed to be the dominant deformation mechanism, while deeper in the upper mantle, dislocation creep may in turn be replaced by diffusion creep. The conditions (depth, temperature) for this transition are still not well determined (Karato and Wu, 1993). If deformation is accommodated by dislocation or diffusion creep, no strain weakening is expected. However, dislocation creep is a strain-rate softening mechanism, which promotes system weakening (Hobbs et al., 1990; Rutter, 1999). This is because diffusion creep has a Newtonian constitutive relation with strain rate proportional to stress, while for dislocation or power-law creep the strain rate is proportional to an exponential power of the applied stress, with the exponent being ~3–4. The development of a system instability (e.g., necking, folding) around a compositional or geometrical heterogeneity is thus promoted by dislocation creep because of the higher sensitivity of the strain rate to stress (Hobbs et al., 1990; Rutter, 1999). Simply, a local stress

* Corresponding author. Tel.: +1 416 978 0833; fax: +1 416 978 3938.
*E-mail address:* boutelier@geology.utoronto.ca (D. Boutelier).

0191-8141/$ - see front matter © 2007 Elsevier Ltd. All rights reserved.
doi:10.1016/j.jsg.2007.10.009

increase around an instability in a system produces a higher strain rate increase if the flow law is of a power-law strain-rate softening type rather than if Newtonian.

In a simplified approach, the bulk rheology of the lithosphere is often described as the competition between brittle failure and dislocation creep, with the mechanism requiring the minimum work under given P/T, stress or strain rate conditions being dominant. In analogue models, a Newtonian approximation is often made for the flow law of rocks in the ductile regime (Weijermars, 1986; Weijermars and Schmeling, 1986; Davy and Cobbold, 1991; Sokoutis et al., 2000; Regard et al., 2003; Fournier et al., 2004; Pysklywec and Cruden, 2004; Cagnard et al., 2006; Cruden et al., 2006). Temperature and compositional variations in the effective viscosity and density of rocks are approximated by using multiple layers of various viscous fluids mixed with granular fillers, plasticine or bouncing putties. However, by using Newtonian materials the deformation rates associated with dislocation creep are underestimated, and little strain localization is possible in the viscous parts of the model. The employment of a ''power-law material'' to model the ductile layers of the lithosphere would allow a better and more natural strain localization process to occur in ''silicone and sand'' analogue experiments.

In this study we investigate the rheology of various filled silicone polymers seeking a strain-rate softening power-law material that is suitable for modelling rock deformation by dislocation creep. It has been shown previously that the addition of granular fillers to a silicone polymer can result in the breakdown of Newtonian behaviour and an increase of the power-law exponent (Poslinski et al., 1988; Leonov, 1990; Walberer and McHugh, 2001; Stickel and Powell, 2005). Similarly, it has been shown that adding oil to plasticine (i.e. decreasing the filler volume fraction) results in a reduction of the power-law exponent (Zulauf et al., 2003). Here we find that high viscosity silicone polymers mixed with plasticine produce strain-dependent materials if the amount of plasticine exceeds 10% of the volume. However, the strain dependency of these materials is only relevant when the shear stress imposed in the material is very small, in which case the material develops a dynamic yield strength. When the shear stress exceeds this threshold, the strain dependency vanishes and the material behaves as a power-law linear visco-elastic fluid with a stress exponent as high as 2.8. Different behaviour is observed for mixtures of low-viscosity silicone polymer with granular fillers. The power-law exponent observed at high stresses imposed on highly-filled low-viscosity silicone polymers never exceeds 1.2. The mechanical properties of the investigated materials are reported in detail and their use in physical modelling is discussed. Two experimental results are presented in which Newtonian and power-law materials are successively used in simple shear experiments. The results demonstrate that the use power-law rheology materials results in better strain localization in analogue experiments. In a companion paper (Schrank et al., in press), the ability of various materials (frictional, plastic, and viscous) to localize deformation is studied in detail using similar simple shear experiments.

For clarity, we hereafter consider a material to be ''linear'' if its mechanical properties do not change with strain. It is then a *linear visco-elastic* material. If a flow law is a linear relationship between stress and strain rate the material is said to be *Newtonian* and if not (e.g., if the flaw law is a power law) it is simply a *non-Newtonian* fluid. A material can thus be ''linear'' (i.e. strain-independent or linear visco-elastic) and ''power-law'' (i.e. stress or strain rate dependent).

## 2. Materials

Silicone polymers mixed with various amounts of granular fillers or plasticine are widely used in analogue experiments. The reason for mixing these materials together is to vary the effective viscosity or the density of a material in order to fulfil scaling relationships. Studies have been made of pure silicone polymers and bouncing putties (Weijermars, 1986), plasticine (McClay, 1976), plasticine softened with added oil (Schopfer and Zulauf, 2002; Zulauf et al., 2003), granular materials (Schellart, 2000; Lohrmann et al., 2003) and mixtures with relatively small amounts of fillers mixed with silicone polymers (ten Grotenhuis et al., 2002). No systematic study has yet been reported on the rheological properties of silicone-based mixtures as functions of filler content. In particular, the mechanical behaviour of highly-filled silicone polymers has not been investigated in view of their use in analogue modelling experiments.

In this study we explore the influence of increasing the amount of filler added to Newtonian pure silicone polymers in order to create a ''power-law'' material suitable for analogue modelling experiments. We acknowledge that it is also possible to design power-law strain-rate softening materials using, for example, mixtures of plasticine and oil (Kobberger and Zulauf, 1995; Zulauf and Zulauf, 2005) or wax and oil (Mancktelow, 1988; Brune and Ellis, 1997).

The silicone polymers used in this study are the ''pure silicone 60,000 cSt fluid'', a polydimethylsiloxane silicone oil hereafter referred as low-viscosity-silicone (LVS), from Clearco Products Co. (Bensalem, PA, USA) and ''Silastic 4-2901'', a polydimethylsiloxane (PDMS) gum manufactured by Dow Corning Co. (Midland, MI, USA). The Clearco silicone oil is a transparent Newtonian viscous fluid with a low viscosity of 57 Pa.s and density of 975 kg/m$^3$. The Dow Corning PDMS has a higher viscosity of $2.5 \times 10^4$ Pa.s and a density of 960 kg/m$^3$. Both silicone polymers are very stable binders, as their mechanical properties do not vary with time or temperature (at the scale of laboratory experiments). The added fillers are a blend of talc and glass bubbles (3M Ltd., S32 Scotchlite), or Harbutt's yellow plasticine. The glass bubbles are low-density (true density of 320 kg/m$^3$) hollow spheres with diameters $\sim$50–100 μm, while the talc powder is composed of 100–300-μm laths with a high true density of 2700 kg/m$^3$. The two granular fillers are first combined together (77% talc and 23% S32 glass bubbles) in order to obtain a homogeneous distribution and are then mixed by hand with the silicone polymer. The resulting mixture is a microscopically homogeneous and stable material since no sedimentation was observed over a period of a several days for the

lowest concentration of filler in the low viscosity silicone polymer to several weeks for the highest concentration.

Plasticine consists of a wax, petrolatum, oil and solvents matrix filled with various combinations of potato starch, calcite, barite and/or kaolinite (McClay, 1976; Schopfer and Zulauf, 2002; Zulauf and Zulauf, 2004). Plasticine is a power-law strain-rate softening material at low shear strain rates. Depending on the fillers, plasticines show steady state flow or a weak to moderate strain hardening (Zulauf and Zulauf, 2004). The plasticine and silicone polymer are slowly mixed by hand. The silicone polymer is progressively incorporated to the plasticine in order to prevent the formation of large pure plasticine flocks. The resulting materials are macroscopically homogenous. Microscopic observation reveals a homogeneous distribution of silicone polymer and micro-flocks of plasticine. The mixtures of plasticine and PDMS are very stable and no sedimentation was observed over a period of months. In this study, the temperature sensitivity of the materials have not been characterised and all measurement are performed at ambient temperature (25 °C). The amount of fillers in the mixtures is quantified by volume % and varies between 0% (pure silicone polymers) and 40%.

## 3. Methods

The mechanical properties of the materials are measured using an AR1000 rheometer (TA Instruments Co.) with parallel-plates geometry (Fig. 1). Various tests are performed to determine the rheological behaviour of the materials.

### 3.1. Dynamic tests

In a dynamic mechanical test, an oscillating (sinusoidal) stress or shear strain function is applied to the sample and the resulting shear strain or stress is measured. For ideal solids following Hooke's law, the shear strain is proportional to the applied stress and the stress and shear strain functions are in phase. In that case, the shift angle ($\delta$) between the two signals is zero (Fig. 2a). If the sample behaves as an ideal fluid and follows Newton's law of viscosity, the rate of shear strain is proportional to the applied stress resulting in stress and shear strain functions with phases shifted by 90° (Fig. 2b). For a visco-elastic material the stress function is complex and can be separated into an elastic stress ($\tau'$), in phase with the shear strain, and a viscous stress ($\tau''$), in phase with the shear strain rate. The elastic stress reflects the degree to which the material behaves as a perfectly elastic solid while the viscous stress is the degree to which the material behaves as a pure fluid. In the case of a visco-elastic material the shift angle between the stress and strain signals ranges between 0 and 90° (Fig. 2c). The material's overall resistance to deformation is the complex shear modulus $G^*$ consisting of an elastic or storage modulus ($G'$) and a viscous or loss modulus ($G''$):

$$G^* = G' + iG'' \tag{1}$$

where $i$ is the imaginary unit. The storage modulus is the ratio of the elastic stress to shear strain while the loss modulus is the ratio of the viscous stress to shear strain. The dynamic moduli can be written as functions of the stress amplitude $\tau_0$, strain amplitude $\gamma_0$, and phase shift angle $\delta$:

$$G' = \frac{\tau_0}{\gamma_0}\cos(\delta) \tag{2}$$

$$G'' = \frac{\tau_0}{\gamma_0}\sin(\delta) \tag{3}$$

The rheometer measures these dynamic moduli as functions of strain, strain rate (frequency), temperature, or time. This provides a robust method for differentiation of the elastic and viscous properties. Whichever modulus ($G'$ or $G''$) is dominant at a particular frequency (equivalent to a shear strain rate) indicates whether the material behaves dominantly elastically or viscously in a process of similar time scale. However, these dynamic functions are defined for a linear visco-elastic material only, and the rheological properties of a visco-elastic material are only independent on shear strain up to a critical value $\gamma_c$, beyond which the behaviour becomes strain-dependent or "non-linear" and the moduli decline.

Dynamic strain sweep tests are carried out to evaluate the linearity or strain dependency of the material. In these tests, a sinusoidal shear strain function is imposed on the sample instead of a shear stress function. The stress-controlled rheometer constantly reads the shear strain function and adjusts the shear stress for the strain function to match the desired sinusoidal function ($\omega$, $\gamma_0$). The amplitude of the shear strain function $\gamma_0$ is progressively increased until the material becomes non-linear while the frequency of the oscillation $\omega$ is kept constant. This allows the determination of the critical strain $\gamma_c$, a measure of the extent of the material's linearity. Subsequently, a dynamic frequency sweep is performed. The frequency $\omega$ is slowly increased while the shear strain amplitude $\gamma_0$ is controlled and kept below the critical shear strain $\gamma_c$. This test

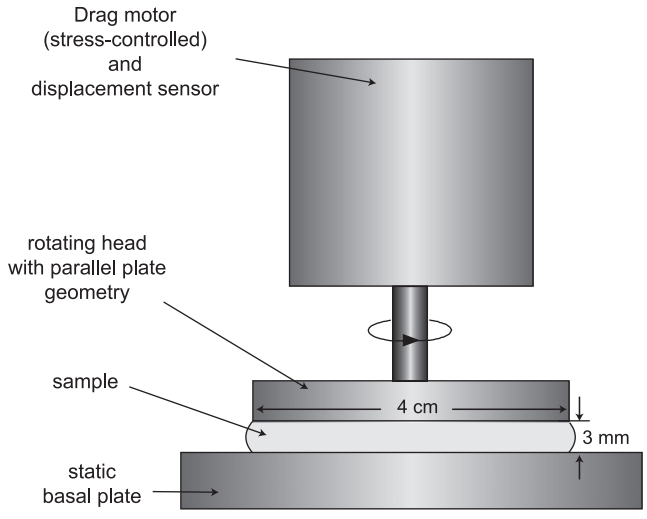


Fig. 1. Sketch of the stress-controlled rheometer. A parallel plate geometry with 4 cm diameter head is used in this study.

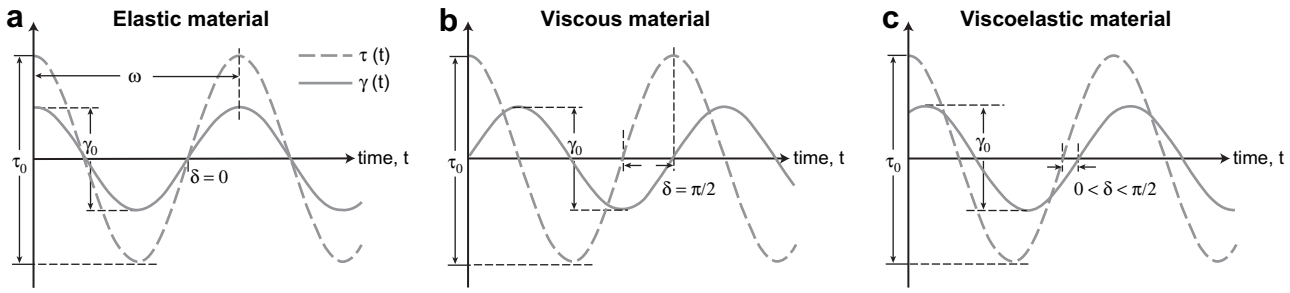


Fig. 2. Sketch of the imposed sinusoidal stress function (dashed) and recorded strain function (bold) in dynamic tests for an ideal elastic (a), viscous (b) and viscoelastic material (c). $\tau(t)$ is the dynamic shear stress function, $\tau_0$ is the amplitude of the stress function, $\gamma(t)$ is the dynamic shear strain function, $\gamma_0$ is the amplitude of the strain function, $\omega$ is the frequency of the imposed oscillation, and $\delta$ is the phase shift angle between shear stress and shear strain.

determines whether the material can be considered purely viscous at the characteristic low shear strain rates used in laboratory modelling. More tests (steady state and transient tests detailed below) are performed to further characterize the mechanical behaviour of the material.

### 3.2. Steady state tests

The steady state flow test is a measure of the material effective viscosity ($\eta_{\text{eff}} = \tau/\dot{\gamma}$) at steady state shear rate. A stress is imposed and the shear strain rate is measured until a steady state has been reached. At this point the rate of shear strain and effective viscosity are recorded and a higher stress is then imposed on the sample. Recorded imposed shear stresses and associated steady state shear strain rate are used to fit a power-law flow law of the form:

$$\dot{\gamma} = \frac{1}{\eta}\tau^n \tag{4}$$

where $\dot{\gamma}$ is the shear strain rate, $\tau$ is the shear stress, $\eta$ is a material constant, and $n$ is the power law exponent. If $n$ is equal to one the material is Newtonian and $\eta$ is then the material's viscosity. This type of test should be performed on visco-elastic materials with a large linear visco-elastic domain because we assume the material properties do not change with strain during the test.

### 3.3. Transient ''creep and recovery'' tests

In a ''creep and recovery'' test, a constant shear stress is imposed on the sample and the resulting shear strain over time is recorded. The stress is then removed abruptly and the ability of the material to recover is recorded (Fig. 3). From the creep test, the viscosity of the sample can be

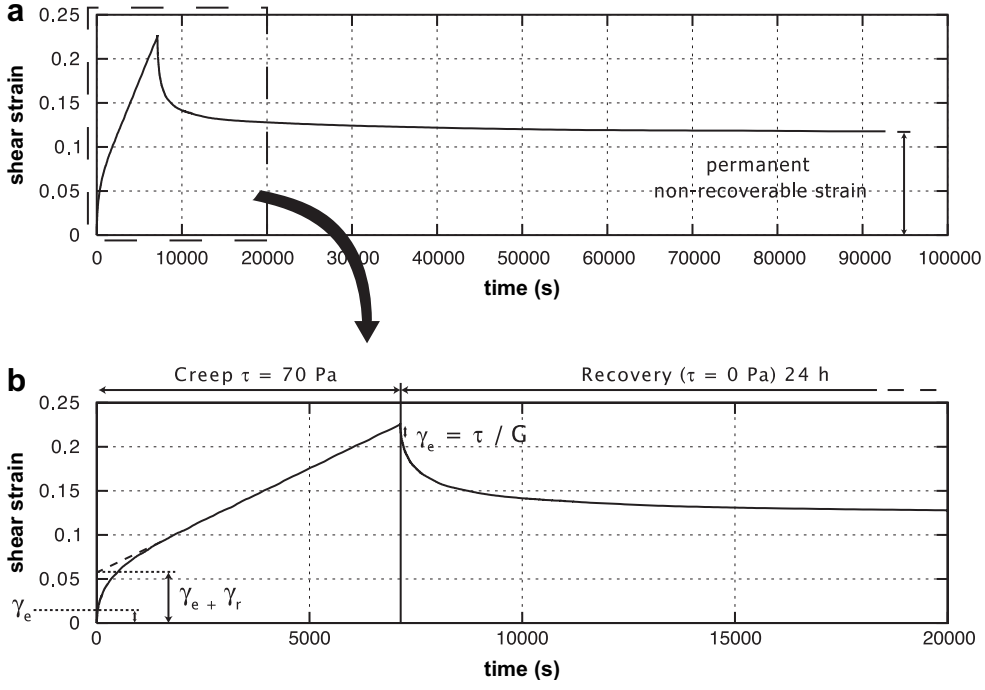


Fig. 3. Examples of shear strain versus time curves obtained during a creep and recovery test for the mixture of PDMS and 20 vol.% plasticine. (a) The duration of the creep varies between 10 and 15 h; the recovery lasts 24 h. (b) The creep and the beginning of the recovery period allow determination of two elastic moduli associated with the instantaneous purely elastic shear strain, $G_e$, and the slowly recoverable visco-elastic shear strain, $G_r$.

determined by dividing the imposed shear stress by the shear strain rate (i.e., the slope of the linear portion of the strain versus time curve). It also provides important information on the elasticity of the sample. The strain versus time curve exhibits three domains: first, a purely elastic and recoverable response of the material to stress; second, a transient visco-elastic response that is eventually recovered slowly when the stress is removed; third, a non-recoverable viscous domain that is either linear (strain-independent) or non-linear.

These tests are used to characterize the elasticity of materials and investigate their behaviour once the critical shear strain has been reached. Beyond $\gamma_c$, the non-linear effective viscosity is recorded as a function of shear strain for each imposed stress. A map of the effective viscosity in stress- and shear strain space is then produced from multiple successive creep tests in order to identify sub-domains of the stress- and shear strain space in which the material behaves quasi-linearly.

## 4. Results

### 4.1. Mixtures of PDMS and plasticine

Strain sweep tests performed on mixtures of PDMS and plasticine (Fig. 4) show that all materials become non-linear after a certain amount of shear strain that is inversely proportional to the volume of plasticine in the mixture. Only the material with the lowest amount of plasticine (10 vol.%) and pure PDMS are linear over a significant range of strain (up to 100% shear strain). We therefore investigated the visco-elastic properties of these two materials with frequency sweep tests (Fig. 5). These tests reveal mainly viscous behaviour for both materials at low frequencies ($G'' >> G'$) but elastic behaviour at high frequencies ($G' >> G''$). For modelling purposes these two materials can thus be considered purely viscous provided the strain rate is kept low ($<10^{-1}\,s^{-1}$). Flow tests yield power-law exponents very close to one for both materials but different viscosity coefficients (Table 1). These results suggest that all mixtures of PDMS and small amounts of plasticine (<10 vol.%) are linear and Newtonian viscous fluids. Hence, it is possible to create a material with a specific viscosity by adjusting the amount of plasticine. However, adding plasticine will also increase the density of the mixture, which is often a crucial parameter in laboratory experiments. One solution to control the density of the final mixture is to incorporate a low-density filler in the mixture. 3M Scotchlite glass bubbles have very small specific gravities (125 to 320 $kg/m^3$, depending on the product) and can be added in small amounts to decrease the density of the mixture without significantly changing the effective viscosity.

For all other materials with more than 10 vol.% plasticine, the rheology is non-linear; in other words the mechanical properties change with strain. To investigate whether this strain dependency is a significant property or can be neglected for some applied shear stresses or shear strain rates, we conducted a series of creep tests on 20 and 40 vol.% plasticine mixtures. Since the results are similar for both materials we present the data for the 20 vol.% plasticine mixture (Fig. 6) and also summarize the flow law obtained for the 40 vol.% mixture.

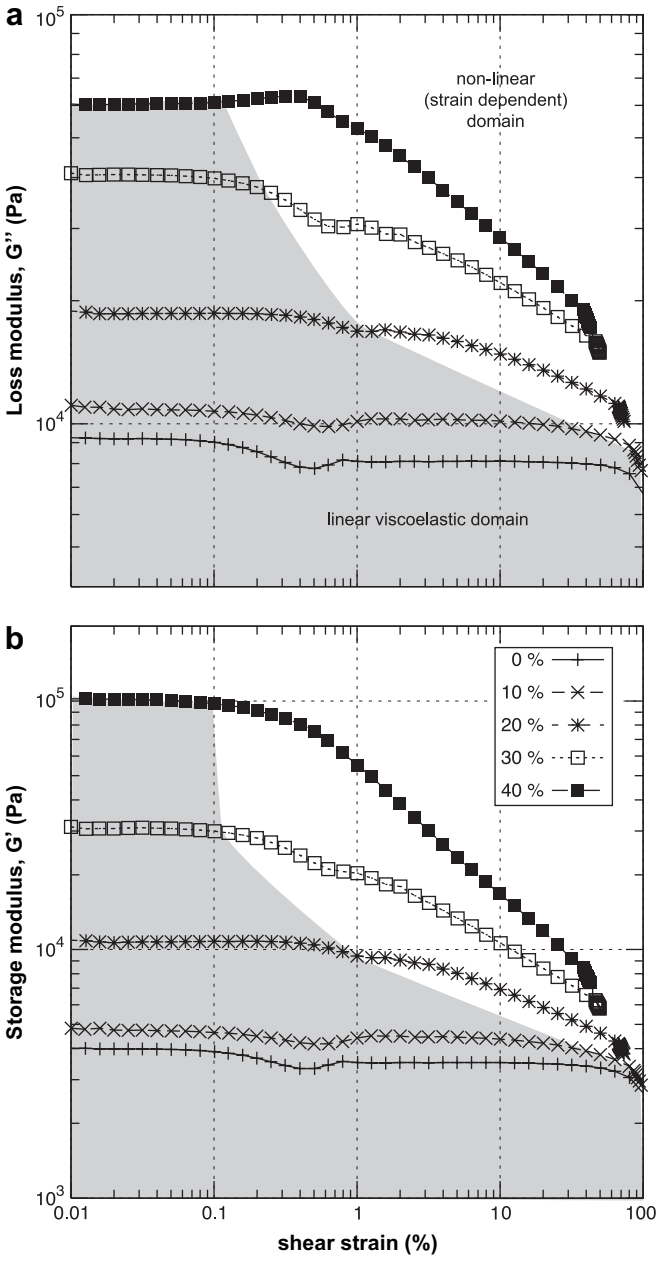


Fig. 4. Results of strain sweep tests for mixtures of PDMS and plasticine. (a) Evolution of the loss modulus ($G''$) with strain for various amounts of filler (volume %). (b) Evolution of the storage modulus ($G'$) with strain for the same amounts of filler. Only the pure PDMS and the 10 vol.% plasticine mixtures are linear visco-elastic materials over a significant range of strain. Oscillation frequency is $10^{-1}\,s^{-1}$.

The shear strain evolution for any applied shear stress is recorded and shear strain rate and effective viscosity are derived (Fig. 6a). Fig. 6b plots effective viscosity in stress-strain space. Shear strain rate is not displayed as a controlling variable since the measurements were made with a stress-controlled rheometer. However, a similar diagram could be obtained if shear strain rate is the controlled variable and shear stress is the dependent one. The viscosity increases with strain when the

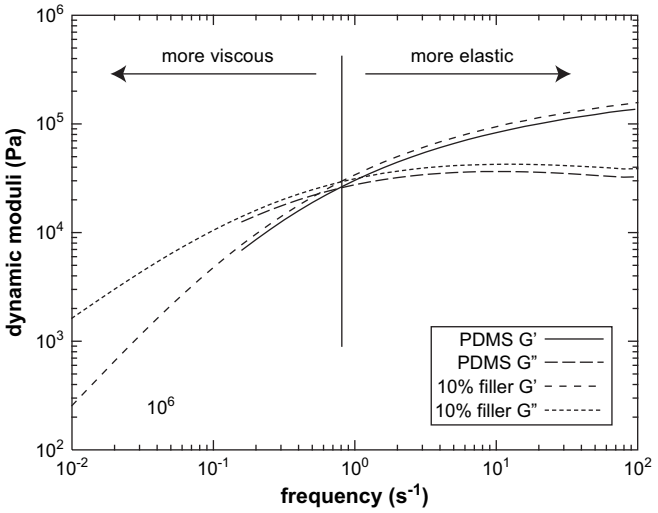


Fig. 5. Results of the frequency sweep tests for the linear visco-elastic mixtures of PDMS and plasticine. Both materials are viscous for low shear rates and are predominantly elastic at high shear rates.

imposed stress is low, but this effect diminishes when the stress is high. For stresses higher than ~70 Pa, the isocontour lines of the effective viscosity clearly show that the material weakens when stress increases but does not harden with increasing shear strain. In this area (right-hand shaded domain in Fig. 6b), the material can be considered "quasi-linear". Assuming the shear strain dependency is negligible for this range of stresses, the slope of the viscosity map at high stresses (>70 Pa) yields a power-law behaviour with an exponent $n = 2.8$. This quasi-linear power-law behaviour has been obtained for a limited range of strain only. Strains below 0.1 are not plotted on Fig. 6b because for small strains the material behaviour is mostly elastic or transient visco-elastic, and not viscous (Fig. 6a). The viscous behaviour could not be investigated with this technique at very high strain because of the high effective viscosity of the material at low stress. In order to produce a deformation map one would need to have creep results with various stresses but similar ranges of strain. However, with a very high effective viscosity ($>1 \times 10^6$ Pa.s) at low stress (Fig. 6b) it is not possible to achieve large strains in reasonable period of time.

At low stresses, the material hardens (i.e. the effective viscosity increases) in a small but significant way and the steep slope suggests that the material is acquiring a dynamic yield stress. The material does not display a classical Bingham yield stress and flows initially even for very low shear stresses. However, as the sample is sheared the material strength increases and when the imposed shear stress is low, the material may stop flowing because of the build up of a dynamic yield stress. The fact that this process does not happen for relatively high shear stresses suggests that the strength increase is related to clustering of particles of plasticine or plasticine fillers in the sample. We speculate that when stress is small, particles may aggregate within the sample creating a cluster that does not yield because shear stress is too low and mechanical jamming prevents the material from further flow. At high stresses, the clusters that may form during flow break down quickly and flow continues (Fig. 7a). As a result, small-amplitude oscillations of the effective viscosity are observed (Fig. 7b). This microscopic mechanical model cannot be verified with our present equipment and further investigation is beyond the scope of the present study.

The elastic properties of the mixture are determined by extrapolating the viscous region of the shear strain versus time curve toward the strain axis and computing a purely elastic shear modulus and a transient visco-elastic shear modulus (Fig. 3). The strain–time curve obtained for the 20 vol.% plasticine mixture submitted to a shear stress of 70 Pa (Fig. 3) gives an elastic shear modulus $G_e = 8 \times 10^4$ Pa and a second modulus $G_r = 2 \times 10^3$ Pa. The Maxwell relaxation times associated with these elastic shear moduli are then 34 and 1375 s respectively, since the viscosity of this material with an imposed shear stress of 70 Pa is $2.75 \times 10^6$ Pa.s.

The 40 vol.% mixture displays a mechanical behaviour similar to that of the 20 vol.% mixture, but since the effective viscosities are higher, the mechanical properties could only be investigated over a very small range of strain (<5%). Nonetheless, we observed an increased power-law exponent of ~4, which suggest that with increasing amounts of plasticine the

Table 1
Measured rheological properties

| Material | Index $n$ | Viscosity (Pa$^n$.s) | Shear rate range (s$^{-1}$) |
|---|---|---|---|
| Dow Corning Silastic gum (PDMS) | $1.013 \pm 2 \times 10^{-3}$ | $2.44 \times 10^4 \pm 2 \times 10^2$ | $1 \times 10^{-6}$–0.1 |
| PDMS + 10 vol.% plasticine | $1.07 \pm 4 \times 10^{-2}$ | $3.9 \times 10^4 \pm 7 \times 10^2$ | $1 \times 10^{-6}$–0.1 |
| Clearco "60,000 cSt" (LVS) | $0.998 \pm 4 \times 10^{-4}$ | $56.2 \pm 1.0$ | $1 \times 10^{-4}$–1 |
| LVS + 10 vol.% filler | $1.006 \pm 1 \times 10^{-3}$ | $79.4 \pm 1.0$ | $1 \times 10^{-2}$–10 |
| LVS + 20 vol.% filler | $1.038 \pm 1 \times 10^{-3}$ | $160.7 \pm 1.0$ | $1 \times 10^{-3}$–10 |
| PDMS + 20 vol.% plasticine | $2.795 \pm 8 \times 10^{-3}$ | $5.8 \times 10^9 \pm 2 \times 10^9$ | $1 \times 10^{-5}$–$1 \times 10^{-4}$ |
| PDMS + 40 vol.% plasticine | $4.6 \pm 1.3$ | $5.88 \times 10^{16} \pm 7.8 \times 10^{15}$ | $4 \times 10^{-8}$–$1 \times 10^{-6}$ |
| LVS + 40 vol.% filler | $1.25 \pm 5 \times 10^{-2}$ | $3.8 \times 10^3 \pm 8.5 \times 10^2$ | 0.01–1 |

The upper part of the table displays the parameters measured for the linear (strain-independent) viscous materials. A power-law of the form $\dot{\gamma} = (1/\eta)\tau^n$ is fitted to more than 50 points in a specific range of shear rates. All linear materials are Newtonian or quasi-Newtonian ($n \sim 1$). The lower part of the table shows the power-law parameters obtained from the creep tests for the strain-dependent materials, which are quasi-linear (strain-independent) in specific sub-domains of the stress-and-strain maps.

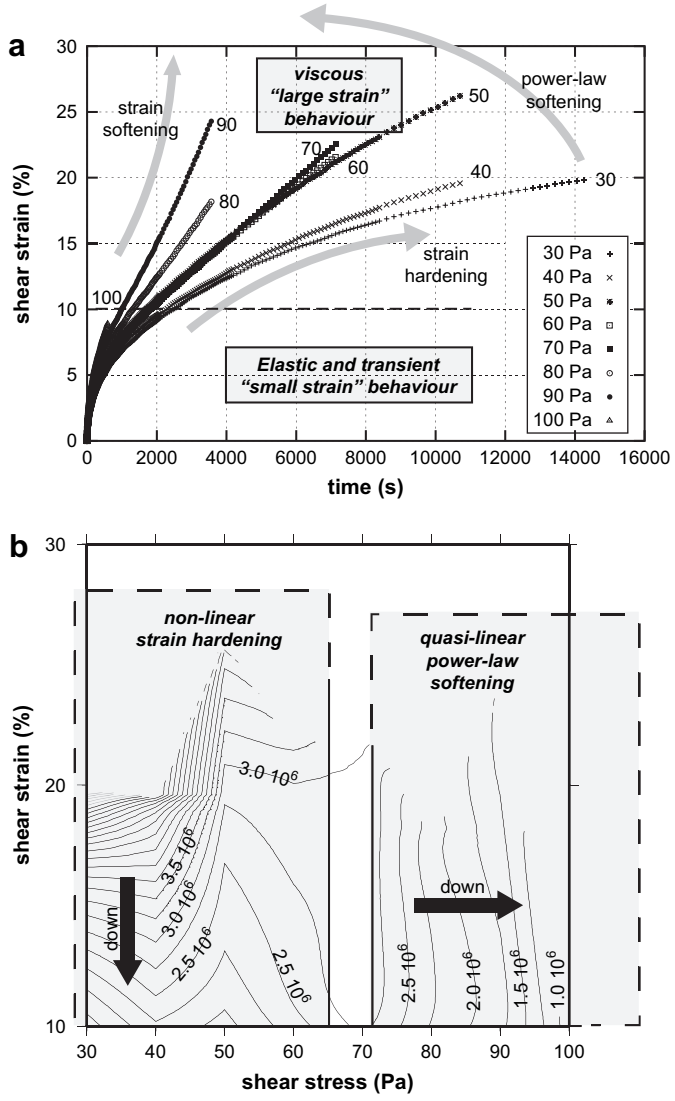


Fig. 6. Results of creep tests for the 20 vol.% plasticine + PDMS mixture. (a) Creep tests reveal visco-elastic behaviour for all imposed stresses. However, the viscous behaviour is not linear since we do not reach a constant viscosity for each stress. Indeed, the viscosity increases with shear strain and decreases with shear stress. (b) Contours of the effective viscosity in shear strain and shear stress space identify two domains (shaded). The left-hand domain shows non-linear (strain-dependent) strain hardening behaviour for small stresses. The right-hand domain reveals quasi-linear (strain-independent) power-law stress softening behaviour for high values of the imposed shear stress. The slope in this domain yields a power law exponent $n$ of 2.8.

power-law exponent of these mixtures approaches the high exponent ($n > 5$) obtained for pure plasticines or plasticine softened with oil (McClay, 1976; Zulauf et al., 2003).

Mixtures of PDMS and plasticine display quite complex behaviours, but have the potential to model rock deformation by dislocation creep with a power-law exponent of about 3. Hence, the typical underestimation of strain rates can be reduced in physical models. These materials should also have a greater ability to localize deformation. To evaluate this hypothesis, we have tested them in simple shear experiments that are reported in a subsequent section of this paper (see also Schrank et al., in press).

One disadvantage of some PDMS and plasticine mixtures for physical modelling may be their very high effective viscosity at relatively low stresses or strain rates. If a material has such a high effective viscosity ($>10^6$ Pa.s), the time scaling factor becomes large, which requires an impractical duration for an experiment. This aspect of the rheology of PDMS and plasticine mixtures suggests that the amount of plasticine should be kept below ~20% vol. to avoid impractically high effective viscosities. To investigate whether we can obtain similar power-law behaviours together with lower effective viscosities, we tested the rheological properties of low viscosity silicone filled with various amount of granular fillers.

### 4.2. Mixtures of low-viscosity silicone polymer (LVS) and granular fillers

Strain sweep tests conducted on mixtures of LVS, talc, and glass bubbles reveal that these materials are non-linear (strain-dependent) if the volume fraction of the filler exceeds 20 vol.% (Fig. 8). Because we started with a lower bound shear strain of 0.1% no linear visco-elastic domain is observed for the mixtures with 30 and 40 vol.% filler, although it might exist for shear strains <0.1%. Frequency sweep tests conducted on LVS and the 10 and 20 vol.% mixtures show viscous behaviour for a large range of frequencies. These mixtures of LVS, talc, and glass bubbles can thus be considered as purely viscous at the typical strain rates of analogue experiments. Flow tests reveal Newtonian and quasi-Newtonian flow with a viscosity that increases with the amount of filler. We did not try to fit the Einstein–Roscoe equation for the viscosity of filled fluids (Roscoe, 1952) since two different kinds of filler with different densities and shapes were used. The viscosities of these materials are given in Table 1.

A mixture with 40 vol.% granular filler has been characterized by creep tests in order to investigate its strain-dependent behaviour. The resulting map of effective viscosity in the stress-strain domain is presented in Fig. 9. As for the strain dependent mixtures of PDMS and plasticine, non-linear or strain dependent behaviour is observed at low stresses. However, the sense of the slope obtained in this case is inverted and the material softens with strain. The material might have a Bingham yield stress as suggested by earlier studies (Poslinski et al., 1988; Leonov, 1990) but this has not been observed here, which suggests it must occur below the minimum stress imposed in the creep tests (30 Pa).

At high imposed stresses the 40 vol.% talc and glass bubbles mixture becomes weaker and quasi-linear (strain-independent). The effective viscosity does not change significantly with strain (right-hand domain in Fig. 9). As for the mixtures with PDMS and plasticine, the slope of the plane toward high stresses yields a power-law exponent. However, for these materials the exponent does not depart significantly from unity. For the 40 vol.% filler mixture we determined an exponent $n = 1.25$, suggesting that it is impossible to reach very high exponents with this kind of material since the volume fraction of 40% is approaching the maximum volume fraction (50–60%).

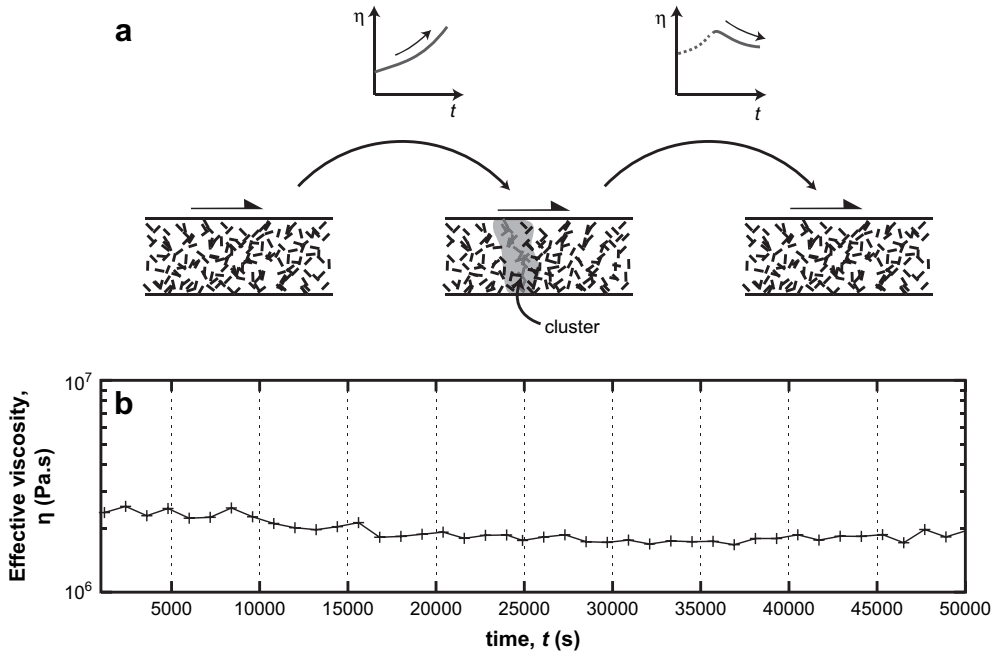


Fig. 7. Sketch of suggested strain hardening/weakening cycle for the mixture of plasticine (20 vol.%) and PDMS. (a) The particles of plasticine cluster with increasing strain until mechanical jamming occurs, leading to an increase of effective viscosity. When the imposed stress is high enough, the particle clusters break and the material weakens, maybe due to development of shape-preferred orientations associated with plastic deformation and rotation of the particles (e.g., White et al., 1980). This cyclic behaviour generates only small amplitude oscillation of the effective viscosity if the imposed stress is high enough. (b) Example of small amplitude oscillations of the effective viscosity recorded with a couette viscometer.

Because these materials are dominantly viscous and the elasticity is very small ($\delta = 80^\circ$ in strain and frequency sweep tests), we did not determine elastic parameters from the creep tests.

## 5. Discussion

In this study we have investigated the mechanical properties of highly filled silicone polymers in order to find a viscous analogue material suitable for modelling rock deformation by dislocation creep. This objective is important because strain localization processes would be better reproduced in laboratory experiments if the viscous flow law for the ductile layers of the model lithosphere were a power-law instead of Newtonian. Since the power law exponent is a dimensionless parameter it should be identical in the model and the prototype (Buckingham, 1914; Weijermars and Schmeling, 1986). For rocks in the lithosphere it should be between 3 and 4 (Kohlstedt et al., 1995). The mixtures of PDMS with 20 to 40 vol.% volume plasticine appear to be suitable because the power-law exponent is close to 3. However, these materials should be used with some restrictions that are elaborated below.

### 5.1. Restrictions

When using PDMS and 20 vol.% plasticine mixture, the imposed shear stress should be above a threshold of 70 Pa, after which the material behaves quasi-linearly. With this minimum level of imposed shear stress the material's effective viscosity is $2.75 \times 10^6$ Pa.s (Fig. 6), which leads to an experimental shear strain rate of $2.5 \times 10^{-5}$ s$^{-1}$. The combination of a high effective viscosity and the need for a relatively high shear strain rate imposes some limitations on the use of this material for lithospheric-scale modelling. The calculation of the shear stress in a particular model cannot be done here since it depends on a variety of parameters characteristic for each setup. However, it is possible to estimate the length scaling factor that should be adopted in order to use this material to model the lithospheric mantle. Let us assume the lithospheric mantle is 120-km thick ($H_p$), has a density ($\rho_p$) of 3300 kg/m$^3$, and an effective viscosity ($\eta_p$) of $1 \times 10^{23}$ Pa.s at a strain rate ($\dot{\gamma}_p$) of $1 \times 10^{-15}$ to $1 \times 10^{-14}$ s$^{-1}$. The experiment is conducted at normal gravity ($g_m = g_p$). Subscript p refers to the parameters in the prototype (i.e. in nature), while subscript m refers to the parameters in the model. A dimensionless ratio can be derived that will ensure that the viscous stress in the material is properly scaled with respect to the lithostatic stress:

$$\frac{\eta\dot{\gamma}}{\rho g H} = \text{Const} \tag{5}$$

Since our material has an effective viscosity ($\eta_m$) of $2.75 \times 10^6$ Pa.s at a strain rate ($\dot{\gamma}_m$) of $2.5 \times 10^{-5}$ s$^{-1}$, and a density ($\rho_m$) of $\sim$1000 kg/m$^3$, the layer thickness $H_m$ is given by:

$$H_m = \frac{\eta_m \dot{\gamma}_m}{\rho_m g_m} \times \frac{\rho_p g_p H_p}{\eta_p \dot{\gamma}_p} \tag{6}$$

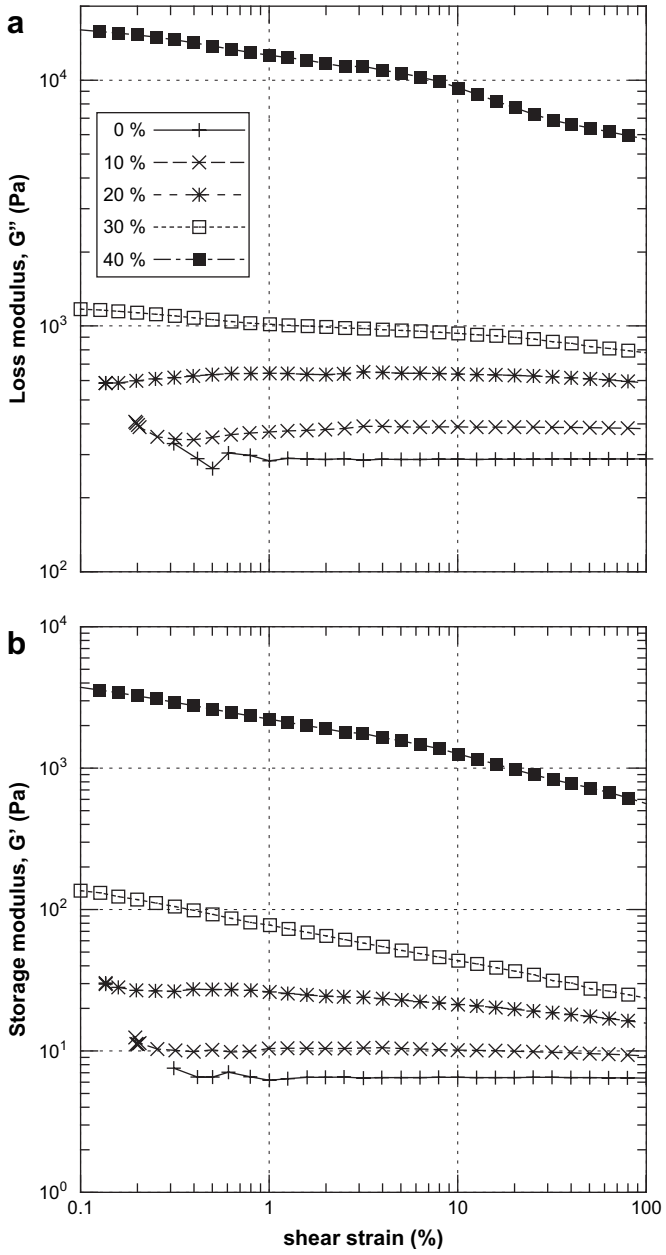


Fig. 8. Results of strain sweep tests for the mixtures of low-viscosity silicone polymer and granular fillers (a blend of talc and glass bubbles). (a) Evolution of the loss modulus ($G''$) with shear strain for various amounts of filler (volume %). (b) Evolution of the storage modulus ($G'$) with shear strain for the same amounts of filler. Only the pure silicon, the 10 and 20 vol.% filler mixtures are linear visco-elastic materials over a significant range of strain. Oscillation frequency is $10^{-1}\ s^{-1}$.

which yields values of 27 to 2.7 cm depending on whether the natural strain rate is assumed to be $1 \times 10^{-15}$ or $1 \times 10^{-14}\ s^{-1}$. The first value of the layer thickness obtained for a lower bound of the natural strain rate is unpractical for laboratory experiments. The second value obtained for the higher bound of the natural strain rate is well within the range of length scales commonly used in analogue experiments. With the strain rate in the experiment being constrained by a minimum rate of $2.5 \times 10^{-5}\ s^{-1}$ required to ensure power-law rheology, we have lost one degree of freedom in the set-up of the experiment compared to previous models performed with Newtonian materials (e.g., Pysklywec and Cruden, 2004; Cruden et al., 2006). This aspect of the scaling also affects the scaling of time. With the aforementioned parameters, 1 Ma in nature is 3.5 h in the model. If we model a process that last 50 Ma (i.e. orogeny), the experiment lasts one week.

It is evident that it would be advantageous to design power-law materials with lower effective viscosities, in order to reduce the duration of the laboratory experiments. It is for this reason we investigated the properties of highly-filled low-viscosity silicone. For practical reasons we used granular materials as fillers. For these materials we observe an increase of the effective viscosities with the filler volume fraction, and power-law rheology for high volume fractions of filler. However, the power-law exponent never exceeds 1.25, even for mixtures containing 40 vol.% of granular fillers. Using these materials does not yield a significant improvement over conventionally employed Newtonian materials. We conclude that an appropriate power-law material with relatively low effective viscosity cannot be designed from a mixture of low-viscosity silicone and granular fillers only. We are currently investigating the properties of materials composed of both high- and low-viscosity silicone polymers mixed with plasticine and low-density granular fillers to overcome this limitation.

Materials made of PDMS and plasticine can however be used for other modelling experiments at intermediate length scales. For example, they can be used to study strain patterns in viscous shear zones in the deeper parts of the crust. Let us assume that a shear zone develops at depth in continental crust in a quartzite. The shear strain rate can be as high as $1 \times 10^{-12}\ s^{-1}$ (Handy, 1994), which gives an effective viscosity of $\sim 1 \times 10^{19}$ Pa.s. Finally, let us assume that the rock has a density of 2800 kg/m$^3$. If we use the 20 vol.% plasticine and PDMS mixture to model this rock, a shear stress higher than 70 Pa is required to be within the power-law domain. If we impose a shear rate of $1 \times 10^{-4}\ s^{-1}$ the effective viscosity is $2.0 \times 10^6$ Pa.s and the shear stress is 100 Pa, which is well within the power-law domain for this material. With a density of 1000 kg/m$^3$ and natural gravitational acceleration the resulting length scaling factor is: 1 cm in the model to 300 m in nature. In the following we present an example of such shear zone modelling experiment in order to illustrate the ability of the power-law material to better localize deformation than in conventional Newtonian fluids.

### 5.2. Strain localization experiments

The modelling setup is similar to that described in the companion paper by Schrank et al. (in press). It consists of a $30 \times 20 \times 4$ cm ($x \times y \times z$) simple shear box that can be filled with various fluids (Fig. 10). A basal cut that is parallel to $x$ in the box centre serves as a sharp velocity discontinuity ($V_x = constant$, $V_y = V_z = 0$) and one half of the box is

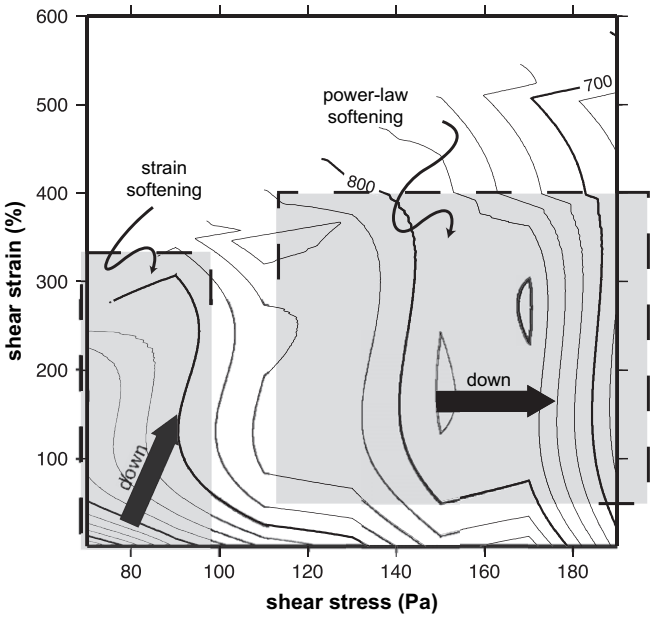


Fig. 9. Results of creep tests for a mixture of LVS + 40 vol.% filler (a blend of talc and glass bubbles) represented as contours of effective viscosity in shear strain- and shear stress space (contouring interval of 25 Pa.s). Two domains are identified (shaded). The left-hand side domain displays a non-linear strain softening behaviour for small stresses. The right-hand side domain reveals quasi-linear power-law behaviour for high values of imposed stress. The slope in this domain yields a power law exponent $n = 1.25$.

displaced horizontally with respect to the stationary second half. Experiments by Schrank et al. (in press) reveal that localization is strongly enhanced by the no-slip basal boundary condition. In order to avoid this effect and to drive the shear zone from the sides rather than the base, we include a 2-cm-thick low-viscosity, high-density corn syrup as a decoupling layer between the sheared material and the bottom of the box (Fig. 10). The sheared layer has dimensions $30 \times 20 \times 0.7$ cm and contains a circular weak seed located in the centre of the box.

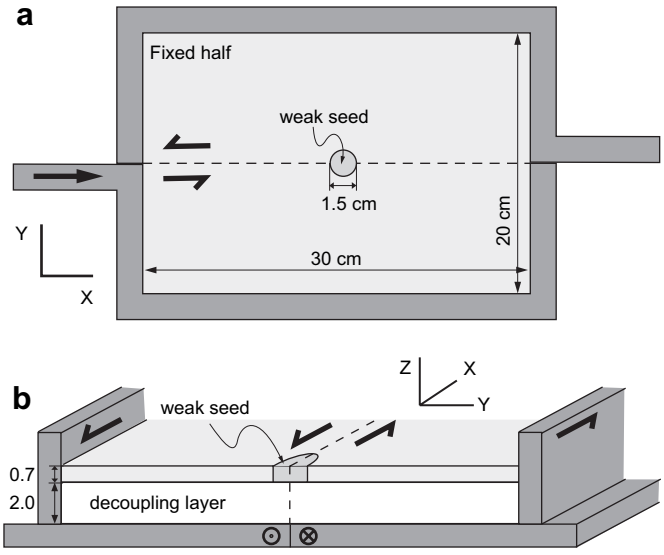


Fig. 10. Sketches of the setup of the shear zone experiments. (a) Surface view, (b) cross-section.

Two experiments are described here. In the first experiment the sheared layer is made of pure PDMS while in the second experiment the sheared layer is made of the 20 vol.% plasticine mixture. In both experiments the weak seed has the same density as the sheared layer and a Newtonian viscosity that is two orders of magnitude lower than the effective viscosity of the sheared layer. A high bulk shear strain rate of $1 \times 10^{-4}$ s$^{-1}$ is imposed in both experiments in order for the 20 vol.% plasticine mixture to be in the "power-law domain" (see Fig. 6b).

Profiles of shear strain $\epsilon_{xy}$ across the shear zone at the final stage of the experiments (total displacement of 5 cm) are presented in Fig. 11c. Particles sifted on top of the sheared material allow determination of the velocity fields using a PIV (Particle Imaging Velocimetry) system (Adam et al., 2005). The velocity gradient d$Ux$/d$y$ is computed for the whole model surface (Fig. 11a,b) and a profile is constructed at the centre of the box in order to avoid boundary effects (Fig. 11c).

The Newtonian material developed a shear strain profile that resembles the parabolic curve obtained when no weak seed is present (Schrank et al., in press). Deformation is only slightly enhanced by the presence of the weak seed (Fig. 11c). The power law material developed two shear zones, both being considerably narrower than the Newtonian shear zone. This unexpected feature (two shear zones instead of one) results from the presence of a second weak seed within the sheared layer related to the model construction. Briefly, an air bubble was trapped between the PDMS + 20 vol.% plasticine layer and the underlying corn syrup during model construction. Despite efforts to remove the air bubble, its effect persisted during the experiment, resulting in the presence of a second weak seed (Fig. 11b).

The description of strain localization also includes on how strain is distributed within the shear zone. To investigate this we use the strain localization intensity parameter $I_{\mathrm{loc}}$ as a measure of the heterogeneity of the shear strain distribution (Schrank et al., in press):

$$I_{\mathrm{loc}} = 1 - \frac{\gamma_{\mathrm{mean}}}{\gamma_{\mathrm{max}}} \tag{7}$$

where $\gamma_{\mathrm{mean}}$ is the mean shear strain integrated over the shear zone width, and $\gamma_{\mathrm{max}}$ the maximum shear strain, usually reached in the shear zone centre. $I_{\mathrm{loc}}$ increases with time in softening materials (progressive localization) and decreases in hardening materials (delocalization). Fig. 11d plots the time evolution of $I_{\mathrm{loc}}$ in both experiments. It is clear that the strain distribution becomes more heterogeneous (more localized) in the power-law material since $I_{\mathrm{loc}}$ increases. This is not the case for the Newtonian material for which $I_{\mathrm{loc}}$ stays almost constant as expected.

The two experiments demonstrate that a power law rheology results in better strain localization in the presence of a weak seed. However, an important difference between the two experiments is due to a point defect inherited from the model set-up. Analogue models are rarely free of such small heterogeneities, but with Newtonian materials these defects usually do not affect the strain distribution. However, when

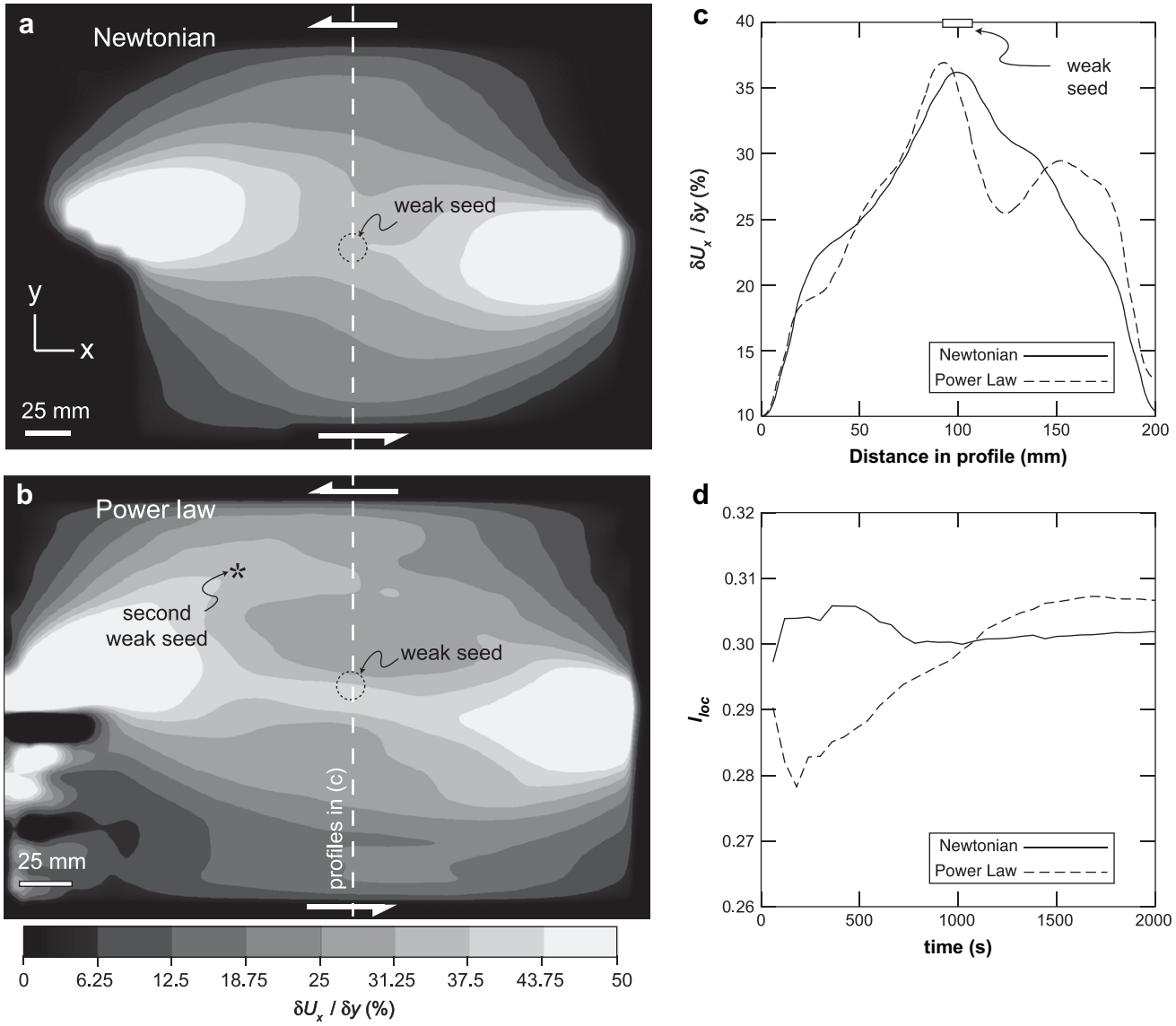


Fig. 11. Results of the shear zone experiments for a Newtonian and a power law material. (a) Map of the shear strain (d$Ux$/dy) in the experiment with Newtonian fluid (pure PDMS) derived by Particle Imaging Velocimetry of the model surface. (b) Map of the shear strain in the experiment with power-law material (PDMS + 0 vol.% plasticine) with location of the weak seeds and profiles shown in c. (c) Shear strain (d$Ux$/dy) profile normal to the shear zone at the end of the experiment (5 cm displacement). (d) Evolution of the strain heterogeneity parameter $I_{loc}$ over time during the two experiments. Increase of $I_{loc}$ for the power law material reveals that within the shear zone, strain is progressively localized in the shear zone centre. See text for further discussion.

using power-law material, this heterogeneity becomes more important and may affect the strain distribution. Such a phenomenon renders the material mixing process and model set-up more difficult if the goal is to use an homogeneous material in order to simplify the analysis of the experiment. However, the sensitivity of strain rate to stress that enhances strain localization around an existing weakness would also allow better investigation of the role of structural inheritance in geodynamic models.

Without significant heterogeneity, the strain profiles in the bubble-free half surface areas (i.e. from 0 to 100 mm in Fig. 11c) look similar. The profile obtained for the power law material is however slightly steeper and narrower. This observation suggests that the power-law flow law is not the most efficient mechanism for strain localization. Strain-softening materials sheared in similar shear zone experiments (Schrank et al., in press) demonstrate that strain softening is more efficient. A combination of both is certainly required to reproduce in analogue models the level of strain localization observed in nature. However, this conclusion should be tempered by the fact that the boundary conditions used in these experiments do not favour system weakening. Localization of shearing in the experiment does not produce a mechanical increase of the stress or strain rate as strain localization does in, for example a necking experiment (ten Grotenhuis et al., 2002). The influence of the power-law rheology on strain localization is more important in models where deformation is not constrained.

## 6. Conclusion

This study of the rheological behaviour of highly filled silicone polymers reveals that adding plasticine or granular fillers to a viscous binder produces mixtures of higher viscosity. If relatively small amounts of filler are incorporated, the resulting material is linear-viscoelastic (strain-independent). Our study confirms that most of the currently used silicone-based analogue materials are Newtonian or nearly-Newtonian viscous fluids at the low stresses or strain rates used in laboratory experiments (ten Grotenhuis et al., 2002). This characteristic makes them more appropriate for simulating natural rocks deforming by diffusion creep. Our data also confirm that the elastic behaviour of these mixtures is negligible at the typically low shear strain rate of laboratory experiments (ten Grotenhuis et al., 2002).

To model rocks that deform by dislocation creep, a higher filler volume should be used. Our investigation of the influence of plasticine and granular fillers suggest that plasticine is more effective for increasing the power-law exponent ($n$). However, these materials should be used with caution since they behave non-linearly. We demonstrate that this non-linear (strain-dependent) behaviour is only significant for low stresses or strain rates. It is therefore possible to design and use a power-law material if the strain rate imposed in the experiments is above a threshold value that must be determined for each compound. Elastic behaviour is shown to be significant for these materials with high volumes of plasticine. However, at large shear strains in kinematically controlled experiments the role of elasticity may be neglected.

The materials presented in this study can be used in a variety of experiments. As an example, we describe two shear zone experiments that illustrate the effect of power-law rheology on enhancing strain localization in the presence of a weak seed. This study suggests that a material made of both high- and low-viscosity silicone with plasticine could provide an appropriate power-law exponent together with a low effective viscosity suitable for modelling an array of ductile creep processes in the lithosphere.

## Acknowledgements

We thank S. Morris, Department of Physics, University of Toronto, for providing access to the rheometer. Constructive comments by reviewers S. ten Grotenhuis and G. Zulauf were appreciated. Funding was provided by the University of Toronto and a Natural Sciences and Engineering Research Council of Canada Discovery Grant to A.R.C.

## References

Adam, J., Urai, J.L., Wieneke, B., Oncken, O., Pfeiffer, K., Kukowski, N., Lohrmann, J., Hoth, S., van der Zee, W., Schmatz, J., 2005. Shear localisation and strain distribution during tectonic faulting-new insights from granular-flow experiments and high-resolution optical image correlation techniques. Journal of Structural Geology 27, 283–301.

Brace, W.F., Kohlstedt, D.L., 1980. Limits on lithospheric stress imposed by laboratory experiments. Journal of Geophysical Research 85, 6248–6252.

Brune, J., Ellis, M., 1997. Structural features in a brittle-ductile wax model of continental extension. Nature 387, 67–70.

Buckingham, E., 1914. On physically similar systems; illustrations of the use of dimensional equations. Physical Review 4, 345–376.

Cagnard, F., Brun, J.-P., Gapais, D., 2006. Modes of thickening of analogue weak lithospheres. Tectonophysics 421, 145–160.

Cruden, A.R., Nasseri, M.H.B., Pysklywec, R., 2006. Surface topography and internal strain variation in wide hot orogens from three-dimensional analogue and two-dimensional numerical vice models. Geological Society, London, Special Publications 253 (1), 79–104.

Davy, P., Cobbold, P., 1991. Experiments on shortening of a 4-layer model of the continental lithosphere. Tectonophysics 188, 1–25.

De Bresser, J.H.P., Ter Heege, J.H., Spiers, C.J., 2000. Grain size reduction by dynamic recrystallization: can it result in major rheological weakening? International Journal of Earth Sciences 90, 28–45.

Fournier, M., Jolivet, L., Davy, P., Thomas, J.-C., 2004. Backarc extension and collision: an experimental approach to the tectonics of Asia. Geophysical Journal International 157, 871–889.

Handy, M., 1994. The energetics of steady state heterogeneous shear in mylonitic rock. Materials Science and Engineering 175, 261–272.

Hobbs, B.E., Muhlhaus, H.-B., Ord, A., 1990. Instability, softening and localization of deformation. Geological Society, London, Special Publications 54 (1), 143–165.

Karato, S.-I., Wu, P., 1993. Rheology of the upper mantle: A synthesis. Science 260, 771–778.

Kobberger, G., Zulauf, G., 1995. Experimental folding and boudinage under pure constructional conditions. Journal of Structural Geology 17, 1055–1063.

Kohlstedt, D.L., Evans, B., Mackwell, S.J., 1995. Strength of the lithosphere: Constraints imposed by laboratory experiments. Journal of Geophysical Research 100, 17587–17602.

Leonov, A.I., 1990. On the rheology of filled polymers. Journal of Rheology 34 (7), 1039–1068.

Lohrmann, J., Kukowski, N., Adam, J., Oncken, O., 2003. The impact of analogue material properties on the geometry, kinematics, and dynamics of convergent sand wedges. Journal of Structural Geology 25, 1691–1711.

Mancktelow, N., 1988. The rheology of paraffin wax and its usefulness as an analogue for rocks. Bulletin of the Geological Institutions of the University of Uppsala 14, 181–193.

McClay, K., 1976. The rheology of plasticine. Tectonophysics 33, 7–15.

Montési, L.G.J., Hirth, G., 2003. Grain size evolution and the rheology of ductile shear zones: from laboratory experiments to postseismic creep. Earth and Planetary Science Letters 211, 97–110.

Montési, L.G.J., Zuber, M.T., 2002. A unified description of localization for application to large-scale tectonics. Journal of Geophysical Research 107, doi:10.1029/2001JB000465.

Poirier, J.-P., 1980. Shear localization and shear instability in materials in the ductile field. Journal of Structural Geology 2, 135–145.

Poslinski, A.J., Ryan, M.E., Gupta, R.K., Seshadri, S.G., Frechette, F.J., 1988. Rheological behavior of filled polymeric systems i. yield stress and shear-thinning effects. Journal of Rheology 32 (7), 703–735.

Pysklywec, R.N., Cruden, A.R., 2004. Coupled crust-mantle dynamics and intraplate tectonics: Two-dimensional numerical and three-dimensional analogue modeling. Geochemistry, Geophysics, Geosystems 5, Q10003, doi:10.1029/2004GC000748.

Regard, V., Faccenna, C., Martinod, J., Bellier, O., Thomas, J.-C., 2003. From subduction to collision: Control of deep processes on the evolution of convergent plate boundary. Journal of Geophysical Research 108, 1–16.

Roscoe, R., 1952. The viscosity of suspensions of rigid spheres. British Journal of Applied Physics 3, 267–269.

Rutter, E., 1999. On the relationship between the formation of shear zones and the form of the flow law for rocks undergoing dynamic recrystallization. Tectonophysics 303, 147–158.

Schellart, W., 2000. Shear test results for cohesion and friction coefficients for different granular materials: scaling implications for their usage in analogue modelling. Tectonophysics 324, 1–16.

Schopfer, M., Zulauf, G., 2002. Strain-dependent rheology and the memory of plasticine. Tectonophysics 354, 85–99.

Schrank, C., Boutelier, D., Cruden, A. The analogue shear zone: from rheology to associated geometry. Journal of Structural Geology, in press, doi:10.1016/j.jsg.2007.11.002.

Schrank, C., Handy, M., Fusseis, F. Multiscaling of shear zones and the evolution of the brittle-to-viscous transition in continental crust. Journal of Geophysical Research, in press, doi:10.1029/2006JB004833.

Sokoutis, D., Bonini, M., Medvedev, S., Boccaletti, M., Talbot, C., Koyi, H., 2000. Indentation of a continent with a built-in thickness change: experiment and nature. Tectonophysics 320, 243–270.

Stickel, J.J., Powell, R.L., 2005. Fluid mechanics and rheology of dense suspensions. Annual Review of Fluid Mechanics 37 (1), 129–149.

ten Grotenhuis, S., Piazolo, S., Passchier, C., Bons, P., 2002. Are polymers suitable rock analogs? Tectonophysics 350, 35–47.

Walberer, J.A., McHugh, A.J., 2001. The linear viscoelastic behavior of highly filled polydimethylsiloxane measured in shear and compression. Journal of Rheology 45 (1), 187–201.

Weijermars, R., 1986. Flow behaviour and physical chemistry of bouncing putties and related polymers in view of tectonic laboratory applications. Tectonophysics 124, 352–358.

Weijermars, R., Schmeling, H., 1986. Scaling of Newtonian and non-Newtonian fluid dynamics without inertia for quantitative modelling of rock flow due to gravity (including the concept of rheological similarity). Physics of the Earth and Planetary Interiors 43, 316–330.

White, S., Burrows, S., Carreras, J., Shaw, N., Humphreys, F., 1980. On mylonites in ductile shear zones. Journal of Structural Geology 2, 175–187.

Zulauf, J., Zulauf, G., 2004. Rheology of plasticine used as rock analogue: the impact of temperature, composition and strain. Journal of Structural Geology 26, 725–737.

Zulauf, J., Zulauf, G., 2005. Coeval folding and boudinage in four dimensions. Journal of Structural Geology 27, 1061–1068.

Zulauf, G., Zulauf, J., Hastreiter, P., Tomandl, B., 2003. A deformation apparatus for three-dimensional coaxial deformation and its application to rheologically stratified analogue material. Journal of Structural Geology 25, 469–480.